Available online at www.sciencedirect.com
SCIENCE DIRECT
Journal of Molecular Catalysis A: Chemical 244 (2006) 46–57
JOURNAL OF MOLECULAR CATALYSIS A: CHEMICAL
www.elsevier.com/locate/molcata

# A comparative study of solid sulfonic acid catalysts based on various ordered mesoporous silica materials

B. Rác [a], Á. Molnár [a,*], P. Forgo [a], M. Mohai [b], I. Bertóti [b]

[a] *Department of Organic Chemistry, University of Szeged, Dóm tér 8, H-6720 Szeged, Hungary*
[b] *Research Laboratory of Materials and Environmental Chemistry, Chemical Research Center, Hungarian Academy of Sciences, P.O. Box 17, H-1525 Budapest, Hungary*

Received 30 March 2005; received in revised form 13 July 2005; accepted 30 August 2005
Available online 4 October 2005

**Abstract**

Acid catalysts based on ordered mesoporous silica materials (MCM-41, HMS, and SBS-15) with covalently anchored propanesulfonic or benzenesulfonic acid groups were synthesized. Six samples were prepared by co-condensation of tetraethylorthosilicate with 3-mercaptopropyltrimethoxysilane or phenyltriethoxysilane in the presence of appropriate templating agents. Six other samples were made by post-synthesis modification of the parent silica materials. Syntheses were followed by oxidation or sulfonation to form surface sulfonic acid groups. Sample characterization was performed by physical (low-angle X-ray powder diffraction, nitrogen adsorption and desorption, diffuse reflectance IR, Raman, NMR, and X-ray photoelectron spectroscopies) and chemical (acid–base titration) methods. Spectroscopic techniques proved successful incorporation of the functional groups. Functionalization of the parent silicas, however, results in changes in structural characteristics (decreasing BET surface areas, changes in pore size distribution, decreasing long range orders). The samples exhibit high activities in various catalytic transformations. Catalysts with anchored benzenesulfonic acid groups of high acid strength and high acid site densities allow the selective synthesis of the cyclic dimer indan product in the dimerization of 2-phenylpropene. 2,3,5-Trimethylhydroquinone diacetate can also be produced in similar high yields in the rearrangement–aromatization of ketoisophorone. Characteristic differences in selectivities are interpreted by taking into account of differences in acid site densities, active site distribution, and the polarity of reactants and catalyst surface. The low activity and selectivity of samples made by grafting in the transformation of ketoisophorone are attributed to the non-random distribution of the acidic functions.


*Keywords:* Mesoporous silicas; Grafting; Co-condensation; Sulfonic acid; 2-Phenylpropene; Ketoisophorone

## 1. Introduction

The large-scale synthesis of industrially important chemicals, as well as the production of fine chemicals often relies on homogenous mineral acids, bases or metal salts, which are applied mostly in stoichiometric amounts. Tightening legislation on the treatment and disposal of excessive toxic waste produced during the separation of the desired products from the reaction medium is forcing industry to consider cleaner technologies and the use of heterogeneous catalysts instead of the often hazardous and corrosive homogeneous counterparts. There are numerous advantages in using heterogeneous catalysts including reduced equipment corrosion, ease of product separation, less potential contamination in waste streams and recycle of the catalyst. For many industrial processes a simple exchange of a well-known homogenous catalyst for a heterogeneous one would eliminate extensive work-up procedures. In addition, the technological processing options are also wider as flow reactors and fixed bed reactors may be applied.

Industrial processes requiring electrophilic catalysts use particularly hazardous and corrosive materials, such as $AlCl_3$, HF, sulfuric acid, and nitric acid [1]. A wide range of solid acids has become available to substitute these aggressive and dangerous materials. Molecular sieves [2] and heteropoly acids [2–4], for example, have been already applied in industrial practice. Commercially available polymeric ion-exchange resins with highly acidic sulfonic acid functional groups, such as polystyrene-based Amberlyst and Dowex materials, are wildly used in var-

* Corresponding author. Tel.: +36 62 544 277; fax: +36 62 544 200.
*E-mail address:* amolnar@chem.u-szeged.hu (Á. Molnár).

1381-1169/$ – see front matter © 2005 Elsevier B.V. All rights reserved.
doi:10.1016/j.molcata.2005.08.043

ious industrial transformations [5–7]. Possible disadvantages, however, are their limited heat stability and the hindered accessibility of the active sites in non-swelling solvents. Because of their hygroscopic nature, absorbed water may also affect catalytic performance. The perfluorosulfonic acid-based resin Nafion-H® also has attractive properties but suffers from a drawback, namely, the activity is limited to the extremely low surface of the polymer beads [7,8]. Recent studies showed, however, that the specific activity of Nafion/silica composites prepared by sol–gel method is several orders of magnitude higher [9,10] and these are efficient catalysts for a number of important transformations [7].

An additional possibility to develop acidic solids is the modification of the surface of suitable support materials. The ideal support or "carrier" should exhibit high thermal and chemical resistance, that is, enhanced stability, and large surface area. This allows a high dispersion of the active species, that is, a high amount of the active centers is accessible for chemisorption. Silica, among other solid carriers, is considered to be a good supporting material. A particularly attractive property is that it has a large number of silanol groups on its surface allowing to covalently bind various organic molecules. These so-called hybrid organic–inorganic materials have attracted growing research interest recently [11,12].

New, even more attractive possibilities arose by the development of various new silica materials with ordered structure. Since their introduction in 1992 [13,14] the mesoporous micelle templated silicas (MTS) are becoming more and more favored for immobilizing homogenous catalysts. One of the best-known examples is MCM-41, which is a structurally well-ordered mesoporous material with narrow pore size distribution between 1.5 and 10 nm, depending on the surfactant cation and a very high surface area up to 1500 $m^2\ g^{-1}$. Since the mesoporosity of these materials may be easily tuned, many organic reactions may be carried out selectively and diffusion problems are minimized. Materials synthesized using neutral templating molecules have, on the other hand, sponge-like, less ordered mesoporous structures. With neutral surfactant molecules, hexagonal mesoporous silicas (HMS) can be synthesized [15–17]. HMS materials also have large surface areas up to 900–1000 $m^2\ g^{-1}$ and a narrow pore size distribution of 3–4 nm depending on the synthesis method, but they exhibit a slightly less ordered structure. Using a poly(ethylene oxide)–poly(propylene oxide)–poly(ethylene oxide) block copolymer (Pluronic 123) as the templating agent, the direct synthesis of SBA-15 can be carried out. SBA-15 silicas show hexagonal mesoporosity with pore sizes up to 8 nm, surface areas up to 800 $m^2\ g^{-1}$, and they have excellent thermal and hydrothermal stabilities [18,19].

A wide range of functional groups, including thiol, amine, epoxide, imidazole, nitrile, alkyl, allyl, and phenyl, have been incorporated into these silica materials [11,20–25]. Two basic processes may be applied. In the post-synthesis modification (grafting or coating), the preformed mesoporous silica is reacted with an appropriate organosilane. In the direct synthesis, co-condensation of the primary building blocks, namely, a silica precursor (e.g., a tetraalkoxysilane) and an organosilane, is carried out in the presence of a suitable surfactant. In either case, further transformation may be necessary to create the required surface functional group.

There are a number of literature data about the functionalization by sulfonic acid group of various silica materials and the catalytic application of the derivatized solids thus prepared. Alkanesulfonic [26–48] or arenesulfonic [44,45,47–51] acid groups were covalently attached to amorphous silica [26–29,31,45,51] and ordered silica materials, namely MCM-41 [30–39,50], HMS [30,31,40,41,47], and SBA-15 [36,41–44,46,48,49], and the materials thus prepared were successfully tested in various acid-catalyzed reactions. In most of these cases, the sulfonic acid function was prepared by the oxidation of the surface-bound propanethiol group. Exceptions are the direct introduction of an arenesulfonic acid group [48,49] and examples when the sulfonation of phenyl-modified amorphous silica [45,51], mesoporous solids [47,50], and polysiloxanes [52] was performed.

The aim of the present study was, therefore, to carry out a comprehensive investigation of various solid acids prepared by synthesizing hybrid organic–inorganic materials of MCM-41, HMS, and SBA-15 structures. Two methods were applied: (i) synthesis by co-condensation of silica materials with surface propanethiol or phenyl function followed by oxidation or sulfonation, respectively and (ii) post-synthesis modification of the three silica materials by grafting through the reaction of 3-mercaptopropyltrimethoxysilane or phenyltriethoxysilane followed by oxidation or sulfonation, respectively. The materials thus produced were characterized by physical and chemical methods and used as catalysts in various organic transformations previously not tested with these types of materials. Catalytic tests were selected to include transformations often applied to characterize acidic solids (Friedel–Crafts alkylation) and reactions (dimerization of 2-phenylpropene, the rearrangement–aromatization of ketoisophorone) never studied before with functionalized mesoporous solid acids.

## 2. Experimental

All materials used except Pluronic 123 (BASF product) were purchased from Aldrich and had purities at least 98% (3-mercaptopropyltrimethoxysilane = 95%).

### 2.1. Synthesis of catalyst materials

#### 2.1.1. Co-condensation

Mesoporous silica materials were prepared with either mercaptopropyl or phenyl groups on their surface using the sol–gel technique. The synthesis is the co-hydrolysis of tetraethylorthosilicate (TEOS) either with 3-mercaptopropyltrimethoxysilane (MPTMS) or phenyltriethoxysilane (PTES) in the presence of hexadecyltrimethylammonium bromide as the templating agent in aqueous NaOH.

In a typical synthesis procedure for MCM-41 materials, the template (hexadecyltrimethylammonium bromide) was dissolved in the given amount of water at 313–318 K, NaOH was added, and then the mixture of the two silicon source (TEOS and MPTMS or TEOS and PTES in molar ratios 4 to 1) was added drop wise. The pH was adjusted to 10 with 50 wt.% $H_2SO_4$ then

the mixture was autoclaved for 168 h at 393 K at autogenous pressure. The resulting suspension was recovered by filtration, washed with water and air-dried. The template was removed by refluxing 4 g templated material in aqueous methanol (538 ml of methanol, 18 ml of 38% HCl, 11 ml of water). The product was washed with methanol then dried in vacuo (393 K, 3 h) [sample designation: MCM41-PrSH(co)]. Following solvent extraction, the thiol group was oxidized to sulfonic acid by $H_2O_2$ in the presence of methanol for 24 h (2.38 ml of 30% $H_2O_2$ in 7.14 ml methanol for 1 g of thiol-functionalized material) at room temperature [31] or at 333 K [27,53]. The oxidized material was resuspensed in 25 ml of 1 wt.% $H_2SO_4$ for 4 h, washed with water, and then dried in vacuo (393 K, 3 h). The sample is designated MCM41-Pr$SO_3$H(co). The sulfonation of the phenyl group was carried out with chlorosulfonic acid in the presence of $CH_2Cl_2$ under reflux for 1 h (25 ml of $CH_2Cl_2$, 5.2 ml of $ClSO_2OH$, 1.5 g of phenyl-functionalized material). After reacting the unreacted chlorosulfonic acid with acetic acid, the product was washed with water to remove all soluble acidic components. Further washing was carried out with (i) 100 ml of $H_2O$–THF (1:1) mixture, (ii) 100 ml of THF, (iii) 100 ml of diethyl ether and, finally the material was dried in vacuo (393 K, 3 h). The sample is designated MCM41-Ph$SO_3$H(co).

Similar co-condensations were performed in aqueous ethanol using dodecylamine template to produce surface-modified HMS samples HMS-Pr$SO_3$H(co) and HMS-Ph$SO_3$H(co). In a typical synthesis procedure, the surfactant was dissolved in ethanol and the desired amount of water was added to get a 44:56 volume ratio of EtOH–$H_2O$. Vigorous stirring was needed to obtain a homogenous solution. After adding the mixture of TEOS and MPTMS (or TEOS and PTES) in a molar ratio of 4:1, the reaction mixture was allowed to react at ambient temperature for 24 h. The TEOS to surfactant molar ratio was 1:0.275. The surfactant was removed from HMS mesostructures by solvent extraction with ethanol by extracting 1.5 g of reaction product with 400 ml of ethanol for 2 days in a Soxhlet-extractor. Oxidation of the thiol group and sulfonation of the phenyl group was performed as described above.

SBA15-Pr$SO_3$H(co) and SBA15-Ph$SO_3$H(co) samples were prepared as follows: 4 g of Pluronic 123 was dissolved with stirring in 125 g of 1.9 M HCl at room temperature. The solution was heated to 313 K and TEOS (0.041 mol) was added to this solution followed by adding the appropriate amount of MPTMS or PTES (0.0328 mol). The mixture was stirred at 313 K for 20 h and aged under static conditions for 24 h at 373 K. The solid products were recovered by filtration and air-dried at room temperature. The template was removed with ethanol under reflux for 24 h (1.5 g as-synthesized material, 400 ml of ethanol). Oxidation of the thiol group and sulfonation of the phenyl group was performed as described above.

#### 2.1.2. Post-synthesis modification

MCM-41, HMS, and SBA-15 silica frameworks synthesized according to the literature [13,17,18] were modified by the grafting technique applying the procedure as described in Ref. [24]. This method, also called coating, results in the formation of oligomeric species and a variety of surface bound species may be developed [54]. In a typical synthesis procedure, 3.5 g of MCM-41 was hydrated by refluxing with 500 ml of water for 3 h. The wet material was suspended in 300 ml of toluene in a Dean–Stark apparatus and $H_2O$/toluene was removed until a translucent suspension was obtained. An excess of MPTMS (20.0 g) was added in order to coat the surface with mercaptopropyl groups. The suspension was stirred for 12 h and refluxed for 3 h. The solid material [designation: *X*-PrSH(g)] was recovered by filtration, washed in a Soxhlet extractor with $CH_2Cl_2$/$Et_2O$ (1:1) for 24 h and air dried. Modification of the surface with phenyl group was performed in a similar way using PTMS (24.5 g). Oxidation of the thiol group and sulfonation of the phenyl group was performed as described above. The six catalysts thus prepared are designated *X*-Pr$SO_3$H(g) and *X*-Ph$SO_3$H(g).

### 2.2. Sample characterization

Low-angle X-ray powder diffraction (XRD) data were acquired on a Philips PW-1820/1830 diffractometer using Cu Kα radiation. The data were collected from 0 to 10° (2$\theta$) with resolution of 0.02 degree.

Nitrogen adsorption and desorption isotherms were measured at 77 K using Quantachrome Nova 2000 system. The data were analyzed using the BJH model. The desorption curve was used to calculate pore size distribution and pore volume.

Diffuse reflectance IR (DRIFT) measurements were made by a BioRad DigiLab FTS 65A/896 spectrometer equipped with a DTGS detector. Spectra were recorded between 400 and 4000 $cm^{-1}$ with resolution of 4 $cm^{-1}$ using the KBr pellet technique (0.015 g of catalyst sample and 300 mg of KBr). Raman measurements were carried out on a BioRad DigiLab FT Raman spectrometer. Spectra were recorded between 0 and 4000 $cm^{-1}$. Solid-state NMR spectra were recorded on a Bruker Avance spectrometer operating at 11.7 T magnetic field ($^{13}C$: 125.7 MHz, $^{29}Si$: 99.3 MHz). Samples were packed in a 4 mm diameter $ZrO_2$ rotor and were spun at 5 kHz speed. Spectra were referenced to tetramethylsilane.

X-ray photoelectron spectra were recorded on a Kratos XSAM 800 spectrometer operated at fixed analyzer transmission mode using Mg Kα1,2 (1253.6 eV) excitation. The pressure of the analysis chamber was lower than $1 \times 10^{-7}$ Pa. Wide scan spectra were recorded in the 100–1300 eV kinetic energy range with 0.5 eV steps and 0.5 s dwell time. High-resolution photoelectron lines of the main constituent elements were recorded by 0.1 eV steps and minimum 1 s dwell time. Spectra were referenced to the energy of the C1s line of the hydrocarbon type adventitious carbon (always present at the surface of the samples), set at 284.6 eV B.E. (binding energy). This corresponds to the referencing to Au 4f7/2 line positioned at binding energy B.E. = 84.0 eV. Quantitative analysis, based on peak area intensities (after removal of the Shirley- or linear-type background), was performed by the Vision 2000 and XPS MultiQuant programs [55,56] using experimentally determined photo-ionization cross-section data of Evans et al. [57] and asymmetry parameters of Reilman et al. [58].

Acid–base titrations as described in [59] were used to measure acid capacity that is the quantity of catalytically active

ingredients of samples. In a typical measurement, 0.5 g of solid was suspended in 50 ml of 0.1 M KCl. The suspension was stirred for 20 min and titrated with 0.2 M KOH in the presence of phenolphthalein.

Microanalyses of the catalyst materials were performed on a Perkin-Elmer 2400 elemental analyzer.

### 2.3. Catalytic test reactions

All reactions were carried out in a round bottom flask equipped with a reflux condenser and stirred magnetically. Temperatures were controlled with an accuracy of ±3 K. Benzene and toluene used in Friedel–Crafts alkylation were stored over sodium wire. Samples withdrawn at intervals from the reaction mixtures were analyzed by capillary GC (Hewlett Packard 5980, 50-m HP1 column). Product identification was made by using GC–MS (HP 5890 GC + HP 5970 mass selective detector), NMR (Bruker DRX 500 spectrometer at 500 MHz, liquid-phase $^1$H spectra), and with comparison with authentic samples. Conversion values were reproducible within ±5%.

Friedel–Crafts alkylation: benzyl alcohol (0.104 ml, 0.001 mol) was reacted with benzene (4.19 ml, 357 K) or toluene (5 ml, 383 K) in the presence of 0.1 g of catalyst and decane as internal standard with magnetic stirring. Competitive studies were performed with benzyl alcohol (0.104 ml, 0.001 mol) and a mixture of benzene (1.78 ml) and toluene (2.13 ml).

The dimerization of 2-phenylpropene (α-methylstyrene, AMS): 0.650 ml (5 mmol) AMS in 5 ml of toluene was stirred at 333 K in the presence of 0.05 g of catalyst. The products are 4-methyl-2,4-diphenylpent-1-ene and 4-methyl-2,4-diphenylpent-2-ene, and the cyclic dimer 1,1,3-trimethyl-3-phenylindan.

Rearrangement–aromatization of ketoisophorone (KIP): ketoisophorone (0.244 ml, 1.4 mmol) was added dropwise to a stirred mixture of acetic anhydride (0.413 ml, 4.3 mmol) and 50 mg of catalyst ($Ac_2O$/KIP molar ratio = 3) under nitrogen. Reactions were run at 318 K.

## 3. Results and discussion

### 3.1. Characterization of the silica structures

Observations acquired by instrumental method (XRD) and results of adsorption–desorption studies are collected in Table 1 and shown in Figs. 1–5 through examples representative of the three silica structures and the synthesis methods.

Low-angle powder XRD patterns of the parent MCM-41 and two MCM-41 samples modified by propanesulfonic and benzenesulfonic acid group using the co-condensation synthesis method are shown in Fig. 1. Sample MCM41-$PrSO_3H$(co) shows three reflections (an intense peak at 2$\theta$ 2.2°, and two weak reflections at 3.8° and 4.4°), corresponding to $d_{100}$, $d_{110}$, and $d_{200}$ spacings of hexagonal symmetry. When compared to the parent MCM-41 structure, only the week reflection at 6.2° is missing. The sample bearing the phenyl group [MCM41-$PhSO_3H$(co)] exhibits only the $d_{100}$ reflection and very similar XRD patterns (not shown) were found for samples made by grafting [MCM41-$PrSO_3H$(g), MCM41-$PhSO_3H$(g)]. This indicates that the long-range ordering of pore arrangement in these three samples is reduced. A small shift of the first diffraction peak to lower 2$\theta$, in turn, is indicative of an increase in pore diameter values (Table 1).

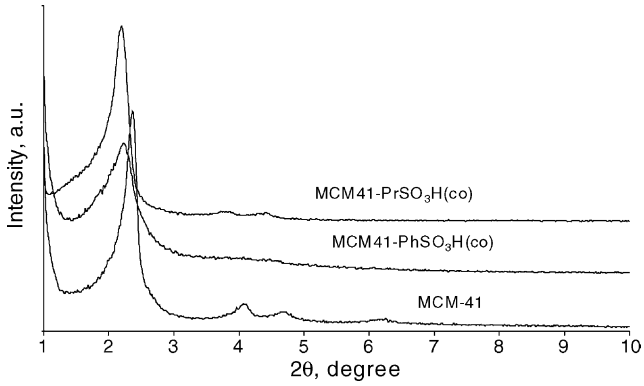


Fig. 1. XRD patterns of MCM-41 samples prepared by co-condensation.

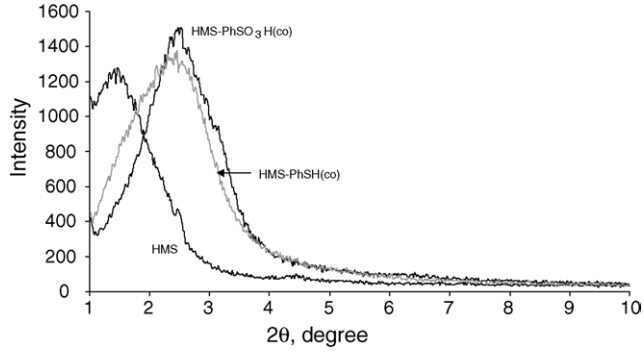


Fig. 2. XRD patterns of HMS samples prepared by co-condensation.

XRD patterns of all HMS samples are very similar having a strong, broad reflection at 2.0–3.0° 2$\theta$ (Fig. 2; two samples prepared by co-condensation are shown). The weak reflection about 4.5° 2$\theta$ of the parent HMS is not present in the functionalized samples. Neither the method of preparation nor oxidation brings about any structural changes. The diffraction peaks, in

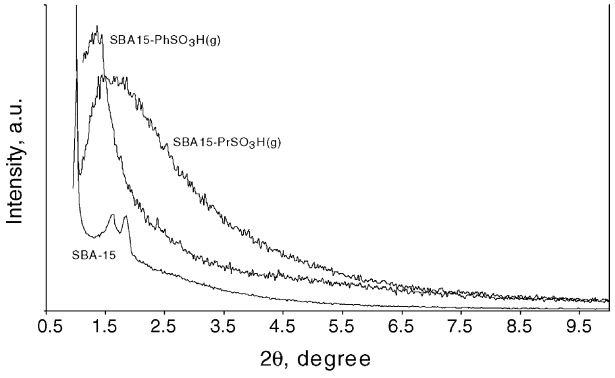


Fig. 3. XRD patterns of SBA samples prepared by post-synthetic modification. (The intensity of the modified samples is multiplied by 10.)

Table 1
Surface characteristics of the parent silica materials and modified samples

| Catalyst | $d_{100}$ | $S_{BET}$ ($m^2\ g^{-1}$) | Pore diameter (nm) | Pore volume ($cm^3\ g^{-1}$) | Acid capacity (mmol $H^+\ g^{-1}$) | Acid site density (mmol $H^+\ m^{-2}$) | Organic content (wt.%) | | |
|---|---|---|---|---|---|---|---|---|---|
| | | | | | | | C | H | S |
| MCM-41 | 4.1 | 1111 | 2.8 | 0.88 | | | | | |
| HMS | 6.2 | 1010 | 5.6 | 0.92 | | | | | |
| SBA-15 | 5.6 | 683 | 6.8 | 1.25 | | | | | |
| MCM41-$PrSO_3H$(co) | 3.8 | 1145 | 3.9 | 0.83 | 1.1 | 0.96 | 11.69 | 3.30 | 7.28 |
| MCM41-$PrSO_3H$(g) | 4.0 | 1068 | 3.9 | 0.87 | 1.1 | 1.03 | 7.45 | 2.69 | 3.57 |
| MCM41-$PhSO_3H$(co) | 4.4 | 738 | 4.1 | 0.84 | 1.5 | 2.03 | 15.65 | 7.47 | 6.00 |
| MCM41-$PhSO_3H$(g) | 4.0 | 853 | 4.0 | 0.81 | 1.6 | 1.88 | 10.36 | 4.64 | 5.24 |
| HMS-$PrSO_3H$(co) | 3.9 | 331 | 3.6 | 0.10 | 0.7 | 2.11 | 10.39 | 2.82 | 7.34 |
| HMS-$PrSO_3H$(g) | 4.0 | 1045 | 2.6 | 0.65 | 0.6 | 0.57 | 6.32 | 2.02 | 2.08 |
| HMS-$PhSO_3H$(co) | 3.9 | 336 | 3.7 | 0.12 | 1.1 | 3.27 | 10.62 | 2.53 | 3.42 |
| HMS-$PhSO_3H$(g) | 3.5 | 974 | 2.4 | 0.54 | 1.1 | 1.13 | 14.07 | 2.60 | 3.48 |
| SBA15-$PrSO_3H$(co) | 7.4 | 236 | 3.4 | 0.72 | 1.1 | 4.66 | 15.89 | 3.80 | 7.61 |
| SBA15-$PrSO_3H$(g) | 5.3 | 340 | 7.0 | 0.98 | 0.4 | 1.18 | 4.76 | 2.72 | 1.46 |
| SBA15-$PhSO_3H$(co) | 6.0 | 261 | 3.4 | 0.51 | 1.2 | 4.60 | 15.39 | 10.85 | 4.05 |
| SBA15-$PhSO_3H$(g) | 6.6 | 671 | 5.3 | 0.23 | 0.5 | 0.75 | 9.75 | 6.03 | 1.68 |

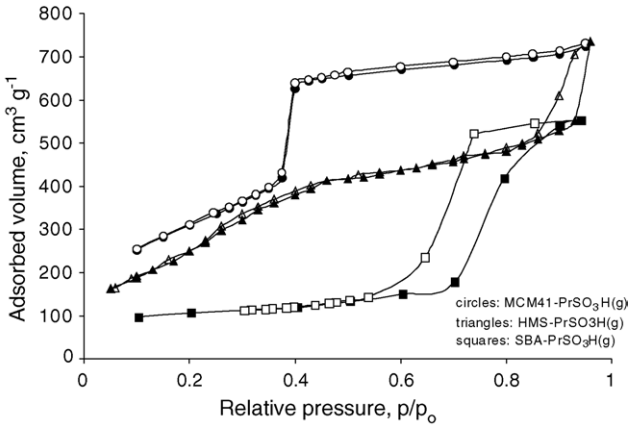


Fig. 4. Nitrogen adsorption–desorption isotherms of samples prepared by post-synthetic modification. Black symbols: adsorption, and open symbols: desorption.

these cases, shift to higher $2\theta$ and a corresponding decrease in pore diameter values is observed (Table 1).

The XRD patterns of modified SBA-15 materials show a similar tendency as in case of MCM-41-based samples. Namely, the higher order (1 1 0) and (2 0 0) reflections, which appear in the parent SBA-15 at 1.6° and 1.7° $2\theta$, are not present (Fig. 3; two samples prepared by post-synthesis modification are shown). This suggests that upon grafting the mesoscopic order decreases slightly, which may indicate that silylation took place inside the mesopores. A significant loss of intensities of the characteristic peaks is observed for samples prepared by co-condensation (not shown). This indicates that the functionalized organosilicon compound applied during synthesis (MPTMS or PTES) hinders the development of the hexagonal structure. Furthermore, the remaining diffraction peak shifts again to higher $2\theta$ with a concomittant decrease in pore diameter values (Table 1).

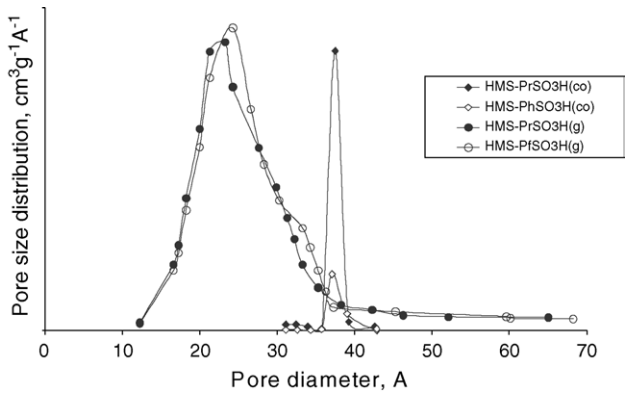


Fig. 5. Pore size distribution of functionalized HMS materials.

Characteristic nitrogen adsorption–desorption isotherms of all three silica materials modified by grafting with propanesulfonic acid surface function are shown in Fig. 4. Two of these [MCM41-$PrSO_3H$(g), SBA15-$PrSO_3H$(g)] exhibit the stepped-shaped isotherms indicative of the pore-filling step. Such curves and sharp inflections at $p/p_0 < 0.4$ and around 0.65 are characteristic of MCM-41 and SBA-15 silicas, respectively [37,60,61]. A pronounced hysteresis occurs in SBA15-$PrSO_3H$(g). In contrast, the pore-filling step for sample HMS-$PrSO_3H$(g) is very shallow. Furthermore, there is a second step at about 0.9 $p/p_0$, which is due to the presence of textural pores [17].

Specific surface areas, average pore diameter, and pore size distributions were calculated by the BJH method. Although this model systematically underestimates the pore sizes it is appropriate for comparative purposes since we are interested in changes brought about by the different synthesis methods. Data summarized in Table 1 indicate that modification of MCM-41 with propanesulfonic acid functions does not affect surface areas, whereas a moderate decrease is observed for samples modified with benzenesulfonic acid groups. Pore diameters, however, increase uniformly, which is in contrast with earlier observations [33,36]. For the other two silica materials, there are no significant differences of data between functional groups. It appears that reaction conditions applied in synthesis (sulfona-

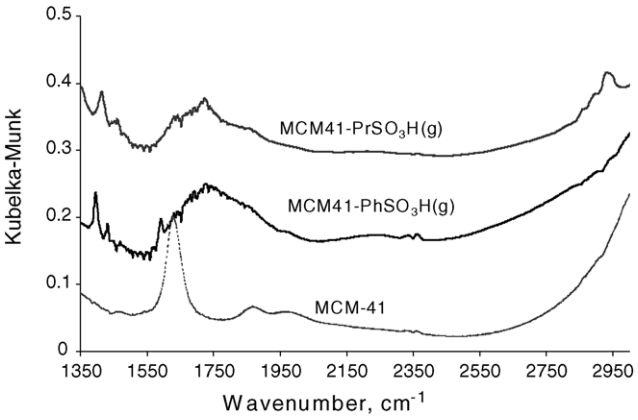


Fig. 6. DRIFT spectra of the MCM-41 framework and two functionalized MCM-41 samples.

tion accomplished in refluxing $CH_2Cl_2$,) affect significantly the structure of MCM-41, which has the most well-defined structure. Synthesis methods, on the other hand, do have effects. BET surface areas and pore diameters of functionalized HMS and SBA materials prepared by co-condensation are significantly smaller than those of the parent silicas and samples made by grafting. Exceptions are functionalized HMS samples where the effect of the latter method on pore diameter is more significant. Furthermore, an interesting difference is found for pore size distribution of HMS samples. As mentioned, samples made by co-condensation have higher pore diameters and very narrow pore size distribution. In addition to larger pore diameters, samples made by co-condensation have very narrow range of pore sizes.

### 3.2. Characterization of the functional groups

The presence of functional groups anchored covalently to the MCM-41, HMS, and SBA-15 silica frameworks are proved by DRIFT, Raman, XPS, and solid-state NMR measurements and the corresponding results are presented in Figs. 6–10. Data shown are representative of the characteristic features of samples with respect to the synthesis methods applied and the two functional groups.

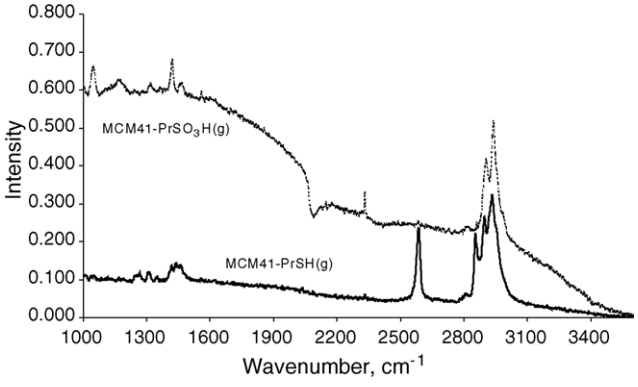


Fig. 7. Raman spectra of sample MCM41-$PrSO_3H$(g) and its precursor containing the thiol function.

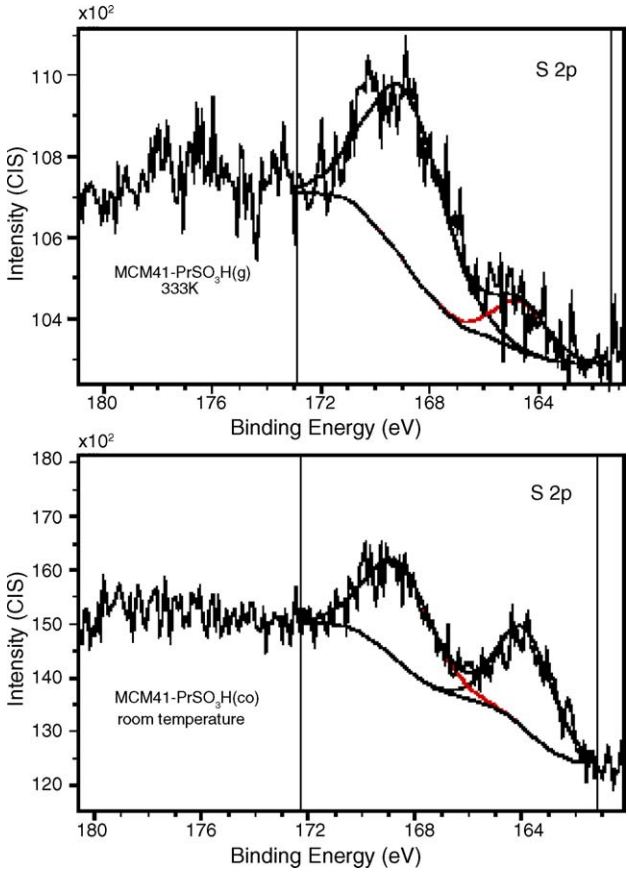


Fig. 8. S2p core-level spectra of MCM41-$PrSO_3H$(co) and MCM41-$PrSO_3H$(g) samples oxidized with $H_2O_2$ at different temperatures.

Fig. 6 shows the DRIFT spectra of the MCM-41 framework and two modified samples containing the propanesulfonic and benzenesulfonic acid functions. The propyl group attached to MCM-41 in sample MCM41-$PrSO_3H$(g) can be identified by the methylene stretching bands in the 2850–2950 $cm^{-1}$ region (2868, 2905, and 2943 $cm^{-1}$) [62]. The corresponding deformation bands are found in the 1410–1470 $cm^{-1}$ region. The intense band at 1415 $cm^{-1}$ is characteristic of the methylene directly bonded to silicon, whereas the band at 1462 $cm^{-1}$ belongs to methylene found in alkanes [62]. The resonance of methylene bonded to sulfur appears as a weak shoulder of this band. The vibration at 1593 $cm^{-1}$ observed in sample MCM41-$PhSO_3H$(g) is characteristic of the phenyl ring. Bands at 1396 and 1417 $cm^{-1}$ found in the two samples (asymmetric stretching of $SO_2$ moieties) confirm the formation of the sulfonic acid species [63].

It is difficult to observe the S–H group by IR spectroscopy due to its low absorptivity. Raman spectroscopy, however, is a suitable technique, as shown by the spectrum of the precursor of sample MCM41-$PrSO_3H$(g) (Fig. 7). The presence of the intense peak at 2585 $cm^{-1}$ is a clear indication of the successful incorporation of the propanethiol function. Furthermore, the disappearance of the S–H vibration upon oxidation by $H_2O_2$ at 333 K indicates its complete transformation into the sulfonic acid group. Further vibrations are at 1043 $cm^{-1}$ and a broad band centered around 1159 $cm^{-1}$ (sulfonic acid group) [37,47].

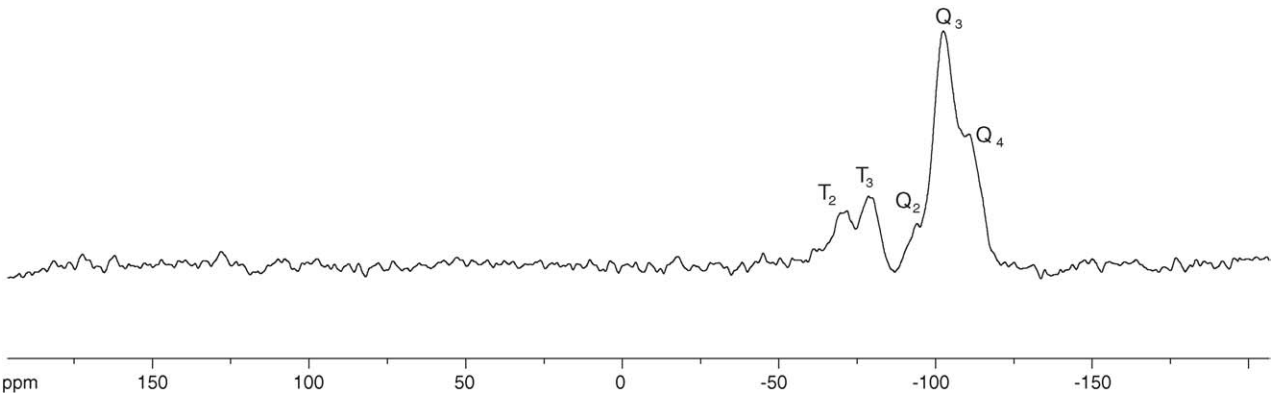


Fig. 9. $^{29}$Si CP-MAS NMR spectrum of sample SBA-PhSO$_3$H(co). Peak positions: −110.8 ppm ($Q_4$), −102.4 ppm ($Q_3$), −94.1 ppm ($Q_2$), −78.6 ($T_3$), and −71.7 ($T_2$).

$CH_2$–S and $CH_2$–Si vibration modes, respectively, are found at 1254 and 1302 cm$^{-1}$ [MCM41-PrSH(g)], and at 1259 and 1312 cm$^{-1}$ [MCM41-PrSO$_3$H(g)].

The oxidation process was further monitored by XPS. S2p core-level spectra of two MCM-41-based samples are given in Fig. 8. A comparison of results indicates that the efficiency of oxidation by $H_2O_2$ at room temperature [27,31] is rather low, that is a substantial fraction of the thiol groups remains intact (Fig. 8). In contrast, near complete conversion can be achieved at 333 K [27,53]. Consequently, samples prepared by this latter procedure were used in catalytic studies.

Spectral characteristics of HMS and SBA-15 samples are practically identical to those of the MCM-41 samples discussed above. The only exception is the presence of a sharp band at 3745 cm$^{-1}$ typical of amorphous silica with isolated silanol groups [64].

The formation of disulfide bridges both during functionalization and oxidation may significantly affect catalytic activities. According to literature, symmetric stretching vibrations in the 500–540 cm$^{-1}$ region in the Raman spectrum [65,66] and signals at 40–41 ppm and 22–23 ppm ($^{13}$C MAS NMR) [30,32,44] are indicative of the presence of disulfide bridges. A careful examination of the corresponding spectra of the six samples with propanethiol function taken before and after oxidation reveals that HMS-PrSO$_3$H(co) is the only sample with detectable disulfide bridge (a weak band at 509 cm$^{-1}$). The lack of disulfide

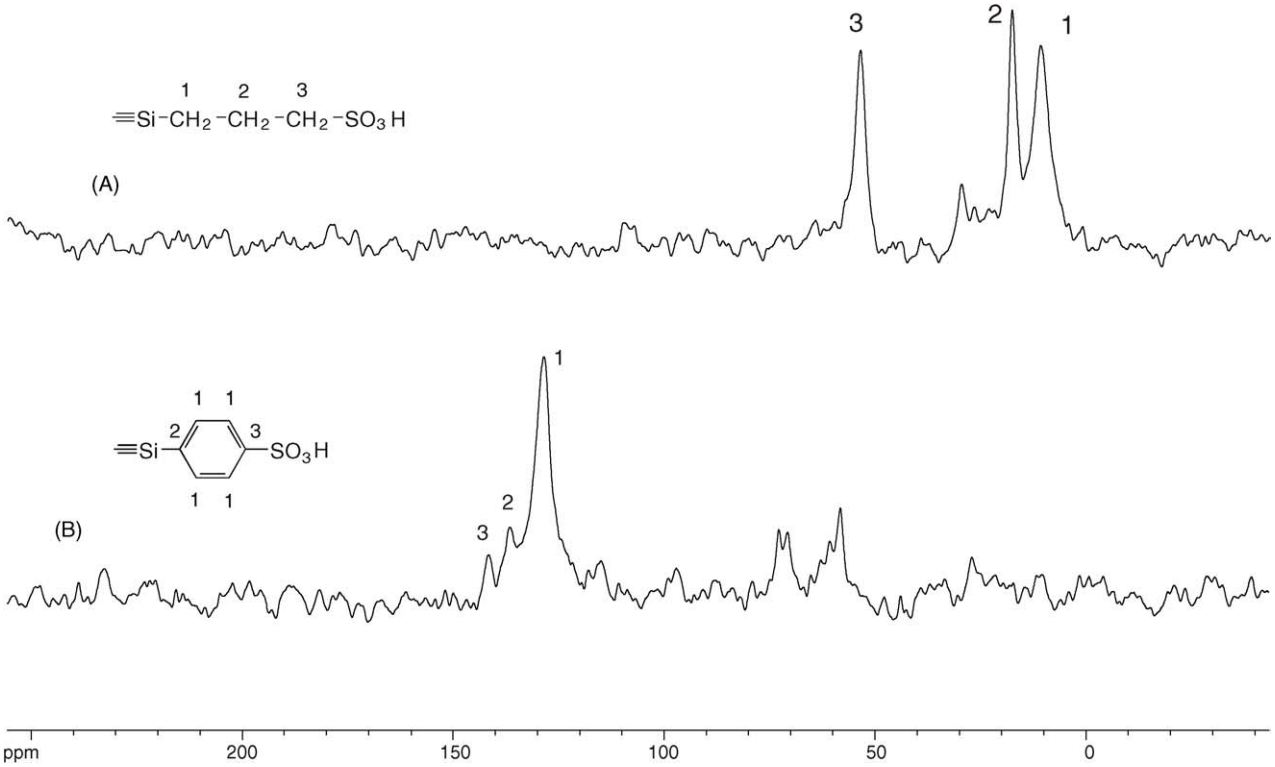


Fig. 10. $^{13}$C MAS NMR spectra of modified MCM-41 samples. (A) MCM41-PrSO$_3$H(co), peak positions: −10.9 ppm (1), −17.7 ppm (2), and −53.6 ppm (3); (B) MCM41-PhSO$_3$H(g), peak positions: −128.5 ppm (1), −136.5 ppm (2), and −141.6 ppm (3).

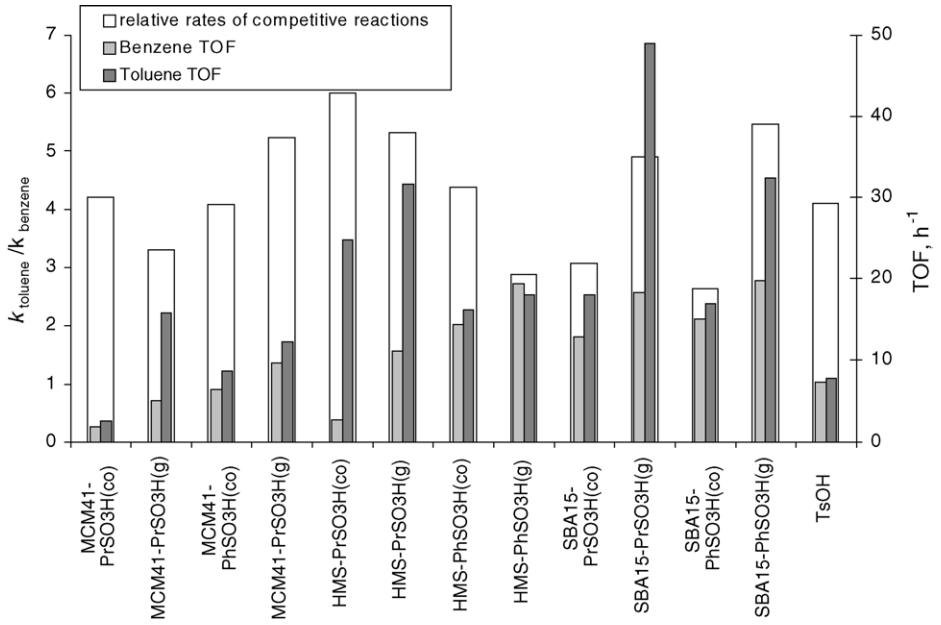


Fig. 11. Rate data and relative rates of Friedel–Crafts alkylation of benzene and toluene with benzyl alcohol (reaction time = 30 min). Shaded bars: rate data measured in individual reactions, empty bars: relative rates determined in competitive reactions with a mixture of benzene and toluene with benzyl alcohol. TsOH: homogeneous reaction performed in the presence of *para*-toluenesulfonic acid.

bridges, in general, is in harmony with other previous observations [31,33,40,60].

As a result of the introduction of functional groups, the cross polarized $^{29}$Si-MAS NMR spectra displayed different signal patterns when compared to the parent silica material [54,67]. The spectrum of SBA15-PhSO$_3$H(co) is shown as a representative example (Fig. 9). The ratio of siloxane $Q_4$ and $Q_3$ sites ($SiO_4$ units) changes to show a much higher intensity of $Q_3$ sites (−102.4 ppm) when compared to the parent SBA-15 silica (not shown). In addition, a signal of $Q_2$ sites appears (−94.1 ppm). Furthermore, new resonances at −78.6 and −71.7 ppm belong to organosiloxane $T_3$ and $T_2$ species, respectively ($SiO_3$ units possessing organic moieties attached to silicon).

In order to identify organic functionalities attached to the surface, $^{13}$C CP-MAS NMR experiments were performed. The solid state cross polarized $^{13}$C spectrum of sample MCM41-PrSO$_3$H(co) with propanesulfonic acid groups on the surface shows three intense signals, which can be assigned to the three carbon atoms of the propyl group (Fig. 10A). The $^{13}$C-spectrum of sample MCM41-PhSO$_3$H(g), in turn, has resonances belonging to the three types of carbon atoms of the aromatic ring (Fig. 10B).

Acid capacities and organic content of samples are also reported in Table 1. It is seen that co-condensation is almost always gives materials with a larger organic content than the grafting process. Further, the large difference found between S content and acid capacity of *X*-PrSO$_3$H(co) samples indicates that a significant fraction of the functional groups are embedded into the silica structure.

### 3.3. Catalytic transformations

The functionalized silica materials characterized above were tested in three reactions: Friedel–Crafts alkylation, dimerization of 2-phenylpropene, and the rearrangement–aromatization of ketoisophorone. Data for these transformations are collected in Figs. 11–13.

Although Friedel–Crafts acylation was the topic in earlier papers applying similar catalysts [28,43,49] there exists only a single example for Friedel–Crafts alkylation over an SBA-15-based catalyst [46]. We have selected the reaction of benzene and toluene with benzyl alcohol to get information about the performance of the catalysts in Friedel–Crafts alkylation. The products were, respectively, diphenylmethane, and a mixture of phenyl-*ortho*-tolylmethane and phenyl-*para*-tolylmethane. Dibenzyl ether was also formed as byproduct.

Overall reaction rates (including the formation of dibenzyl ether) collected in Fig. 11 show that as expected, toluene, an activated aromatic compound, always exhibits higher reactivity when rates of the two aromatic compounds over the same catalyst are compared [the only exception is HMS-PhSO$_3$H(g)]. Even more reliable data can be acquired in competitive studies with a mixture of the two reactants. The ratios $k_{toluene}/k_{benzene}$

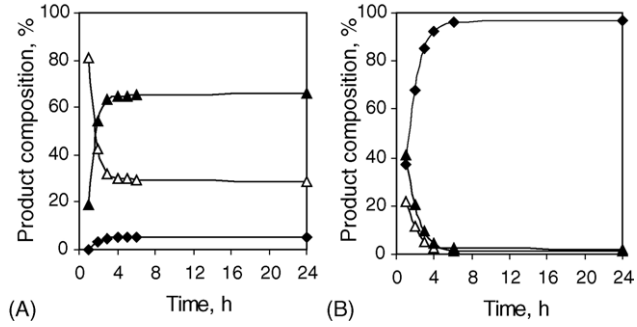


Fig. 12. Time dependence of product composition in the dimerization of AMS. (A) MCM41-PrSO$_3$H(co), (B) MCM41-PhSO$_3$H(co). (▲) **1-P**, (△) **2-P**, (♦) **indan**.

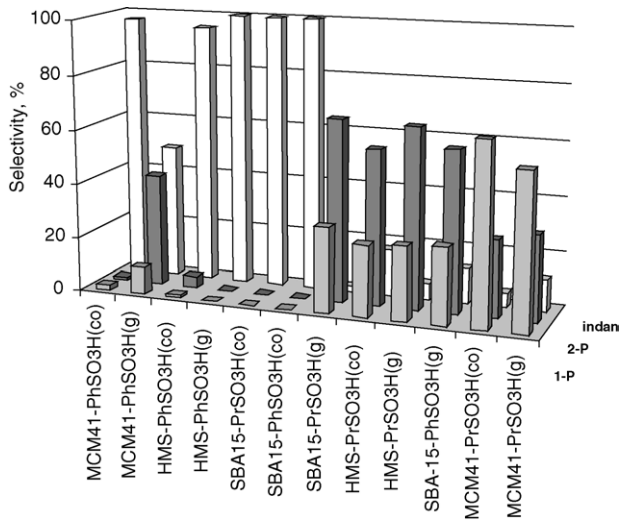


Fig. 13. Selectivities in the dimerization of AMS (reaction time = 24 h). **1-P**: 4-methyl-2,4-diphenylpent-1-ene; **2-P**: 4-methyl-2,4-diphenylpent-2-ene; **indan**: 1,1,3-trimethyl-3-phenylindan.

(considering only alkylation products) are in the range between 2.6 and 6. The selectivities of the regioisomers (*ortho*- and *para*-substituted compounds) in the benzylation of toluene are close to unity. All these features, that is low substrate and low positional selectivities, are characteristics of a usual Friedel–Crafts alkylation reaction [68]. These observations are very similar to the results found in a homogeneous reaction performed in the presence of *para*-toluenesulfonic acid (Fig. 11, TsOH).

The side-reaction, the formation of dibenzyl ether is also worth discussing. Under homogeneous conditions (TsOH) dibenzyl ether was not detected, whereas high amounts (up to 30% selectivity) were detected over the mesoporous catalysts. Two effects may account for the observations. (i) Benzyl alcohol with the polar hydroxyl group is capable of a preferential adsorption on appropriate surface active sites; that is, a partitioning effect is certainly involved using heterogeneous catalysts. (ii) Furthermore, the presence of dibenzyl ether indicates that benzyl alcohol successfully competes for the electrophile with the aromatic reactants. This shows that benzyl alcohol is not fully transformed into the reactive electrophilic intermediate. Indeed, when alkylations with increased catalyst quantities were performed, alkylation selectivities did improve. For example, using 0.3 g of SBA15-PhSO$_3$H(co) catalyst in the alkylation of benzene instead of 0.1 g, the original alkylation selectivity versus ether formation of 61/39 increased substantially to 73/21.

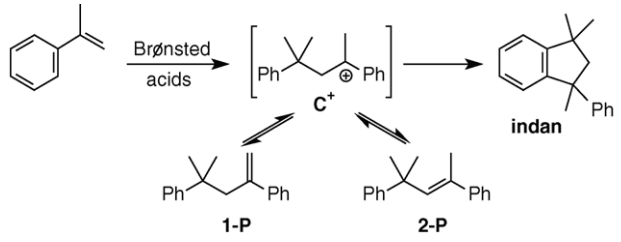


Scheme 1. Dimerization of 2-phenylpropene (AMS).

Dimerization of 2-phenylpropene (AMS, Scheme 1) is an important process because the product open-chain and cyclic dimers find application in polymer production and in the electronic industry [69]. Catalysts were tested under various reaction conditions to achieve appropriate selectivities [70–73]. Our previous study with silica-supported Nafion-H prepared by ball milling showed that the accessibility of the active sites by the reacting molecules is a crucial factor determining selectivities [74].

We have found high activities for all catalyst samples ensuring complete conversion in a short reaction time [1–3 h; the only exception is HMS-PrSO$_3$H(g) giving only 62% conversion in 24 h]. Selectivities, in turn, differ considerably and change significantly with increasing reaction time to have a final product distribution in 24 h (Fig. 12). It is known from previous studies that the dimeric carbocationic intermediate (**C$^+$**) plays a crucial role in the process: it is transformed into the two isomeric pentene derivatives (**1-P** and **2-P**) in equilibrium reactions, whereas the cyclic dimer 1,1,3-trimethyl-3-phenylindan (**indan**) is formed irreversibly [69]. On the basis of time dependence of selectivities, 4-methyl-2,4-diphenylpent-1-ene is the primary product, which undergoes isomerization to yield the isomeric 2-alkene and, finally, the indan derivative is formed.

All catalysts exhibit high activities (conversions exceeding 90% are achieved in about 1–3 h reaction time; the only exception is HMS-PrSO$_3$H(g), which gives only 62% conversion at 24 h). However, significant differences are found in selectivities. Two characteristic examples are shown in Fig. 12. A final product distribution is usually achieved in 24 h.

An analysis of selectivities (Fig. 13) and physical characterization data (Table 1) shows that catalysts can be divided into two groups: six catalyst samples give the two alkene isomers as major products, whereas in the presence of the other six catalysts the indan derivative is obtained with high selectivities [the only minor exception is MCM41-PhSO$_3$H(g), which exhibits somewhat lower selectivity].

Five of the six catalysts producing **indan** with high selectivity are functionalized with benzenesulfonic acid group. Clearly, catalyst samples with higher acid strength exhibit the best performance in this reaction. Moreover, all six catalysts, which afford the cyclic dimer with very high selectivities have high acid site densities. High concentration of acidic sites of high acid strength, obviously, ensures the fast isomerization of the linear alkene dimers to the cyclic indan product.

Of the other six samples, two propyl-modified MCM-41 catalysts [MCM41-PrSO$_3$H(co), MCM41-PrSO$_3$H(g)] yield the primary product alkene **1-P** as the main product. These two samples have medium acid capacity and the highest surface area of all samples, that is, rather low acid site densities. The four catalyst samples, which give the other alkene isomer (**2-P**), in turn, have medium specific surface concentration of the acid sites and the lowest acid capacities (0.4–0.7 mmol H$^+$ g$^{-1}$, Table 1). However, the nature of the silica structure does not appear to have any effect on catalytic performance.

As disclosed earlier [69,73] the selectivity of dimerization can be affected by temperature. Indeed, lowering the reaction temperature from 333 to 318 K results in significant changes in

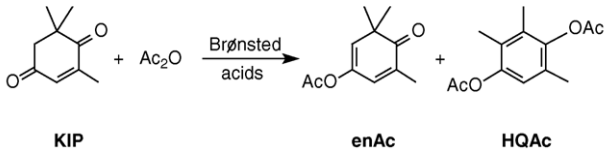


Scheme 2. Rearrangement–aromatization of ketoisophorone (KIP).

product selectivities. For example, the high indan yield (76%) over MCM41-PhSO$_3$H measured at 333 K decreased significantly to 8% when the reaction was performed at 318 K. In parallel, the overall yield of the isomeric alkenes increased from 24% to 92% (7% **1-P** and 17% **2-P** versus 39% **1-P** and 53% **2-P**).

Since all but one catalysts exhibited high but uniform activities in the above process, we have searched for another reaction, which is more demanding and allows to differentiate between the catalysts on the basis of their activities. Rearrangement–aromatization, also known as dienone–phenol rearrangement [75] proved to be a suitable choice. Ketoisophorone (**KIP**), when treated with acetic anhydride in the presence of Brønsted acids, yields 2,3,5-trimethylhydroquinone diacetate (**HQAc**), which is an intermediate in the production of α-tocopherol (Scheme 2). Nafion systems have recently been found to show high activities in this transformation [76].

Significant differences were found with respect to the activity of the 12 catalysts studied and selectivities also differ considerably. Two characteristic examples illustrating two different catalyst performances are shown in Fig. 14, whereas Fig. 15 gives a summary of the results observed on all 12 catalysts. The most active samples produce **HQAc** as the main product. This transformation takes place with the involvement of a carbocationic intermediate and requires a 1,2 methyl migration. Catalysts with lower activity, in turn, yield the enol monoacetate (**enAc**) in a process of simple enolization–acetylation (Fig. 13).

Correlations between activities and selectivities are clearly seen. Selectivity of the formation of **HQAc**, the product of a more demanding reaction, increases with increasing catalytic activity (conversion). Formation of the enol acetate, in turn, shows an inverse correlation: samples with low activity produce the highest amount of **enAc**.

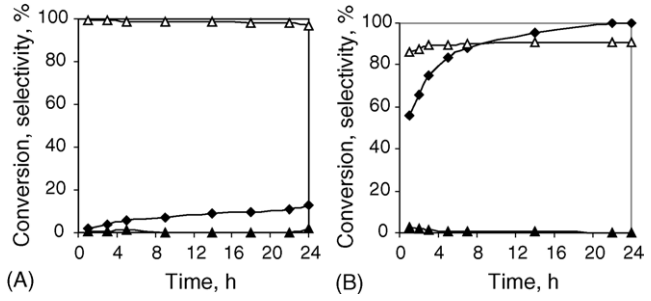


Fig. 14. Time dependence of product composition in the rearrangement–aromatization of KIP: (A) HMS-PrSO$_3$H(g), (B) HMS-PhSO$_3$H(g). (△) **enAc**, (▲) **HQAc**, and (♦) conversion.

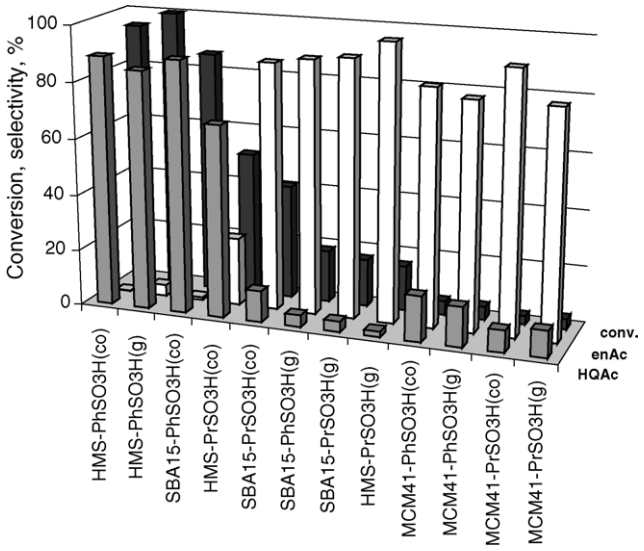


Fig. 15. Conversions and selectivities in the rearrangement–aromatization of ketoisophorone (reaction time = 24 h): **enAc**: enol monoacetate; **HQAc**: 2,3,5-trimethylhydroquinone diacetate.

It is found again that three of the best catalyst samples exhibiting the highest activity and affording **HQAc** in high yields are those with anchored benzenesulfonic acid groups of higher acid strength. Moreover, two of these are also characterized by high acid site density. Four samples with propanesulfonic acid functions and the lowest acid site density [MCM41-PrSO$_3$H(g), MCM41-PrSO$_3$H(co), HMS-PrSO$_3$H(g), and SBA15-PrSO$_3$H(g)], in turn, are found at the other end of the spectrum. Catalytic performance of some of the other samples, however, is more difficult to explain, particularly that of the other three catalysts with benzenesulfonic acid groups [MCM41-PhSO$_3$H(g), MCM41-PhSO$_3$H(co), and HMS-PrSO$_3$H(co)]. Obviously, this requires taking into account other factors.

In studies with highly sulfonated resins, acidity enhancement was observed and associated with networks of sulfonic acid groups [77,78]. It was argued that interacting neighboring sulfonic acid groups in clusters may exhibit higher acid strengths than isolated functions. Enhanced activity of SBA-15 functionalized with sulfonic acid groups in a pairwise arrangement was also observed by Dufaud and Davis [44]. The phenomenon was attributed to the cooperative effect between two proximal functional groups. In a recent work, Koujout and Brown found differences in acid strengths of sulfonic acid modified polystyrene resins and mesoporous silicas (HMS and SBA-15) in various solvents [43]. Here this was interpreted by uneven distribution of functional groups accentuated by solvent polarity. Furthermore, it is known that the active site distribution of these silica materials is not necessarily uniform, particularly if they are made by the grafting technique. It was shown by Brunel et al. [79] that mainly the hydrophobic portion of the surface with isolated silanol groups and surface siloxane bridges participates in the grafting process. As a result, interacting hydrogen-bonded silanol groups forming hydrophilic networks remain mostly intact. The grafting technique, consequently, produces materials with islands of active centers surrounded by hydrophilic patches. The active

site distribution of catalysts made by co-condensation, in turn, is considered to be more random.

Such effects certainly play a role in the catalytic performance of our samples. It is seen that catalysts made by co-condensation usually exhibit better performance. This is particularly evident in the test reaction of **KIP**: five of the six catalysts made by grafting exhibit low activity and produce only the simple monoacetylation product (**enAc**). It may be surmised, that the highly polar molecules participating in this reaction and the intermediate **enAc** may be strongly adsorbed on the sulfonic acid functions and the surrounding hydrophilic areas blocking the active sites. More random active sites characteristic of catalysts made by co-condensation may be more accessible to reacting molecules. Similar effects found in acetalization reaction over sulfonic acid functionalized FSM-16 silica have recently been described [80].

Such effects are less straight-forward in the transformation of AMS, which is a less polar molecule. Nevertheless, four of the six samples not able to induce the formation of the cyclic dimer indan to significant degrees are made by grafting.

## 4. Conclusions

Mesoporous ordered silica materials (MCM-41, HMS, and SBS-15) were successfully derivatized with covalently anchored propanesulfonic or benzenesulfonic acid groups applying co-condensation or post-synthesis modification (grafting). Physical characterization techniques indicate that functionalization affects the structural characteristics of the parent silica materials manifested by decreasing BET surface areas and long-range orders, and changes in pore size distribution.

The results of catalytic performance acquired in various test reactions indicate that a combination of subtle differences in surface characteristics and the polarity of reacting molecules may have significant effect on catalytic activities. It is found that catalysts made by co-condensation and functionalized by benzenesulfonic acid groups are more active and more selective.

The catalysts with anchored benzenesulfonic acid groups of high acid strength afford the cyclic dimer indan product in the dimerization of 2-phenylpropene with high selectivity. In addition, these samples have high acid site densities thereby ensuring the fast isomerization of the linear alkene dimers to the cyclic product.

Some of the same catalyst samples functionalized with benzenesulfonic acid groups exhibit similar good catalyst performance in the rearrangement–aromatization of ketoisophorone to form 2,3,5-trimethylhydroquinone diacetate. Five catalysts made by grafting exhibit low activity and produce only the simple monoacetylation product (**enAc**). This may be attributed to the non-random distribution of the acidic functions, which are surrounded by hydrophilic areas resulting in the blocking of the active sites by strongly adsorbing reactants and intermediates.

## Acknowledgments

XPS characterization was performed in the ESCA Laboratory of the OTKA Materials Science Measuring Center (Budapest). We are most grateful for financial supports from the Hungarian National Science Foundation (OTKA grants T042603, TS044690 and M041532).

## References

[1] G.A. Olah, Á Molnár, Hydrocarbon Chemistry, 2nd ed., Wiley, Hoboken, 2003.
[2] Y. Izumi, K. Urabe, M. Onaka, Zeolite, Clay and Heteropoly Acid in Organic Reactions Kodansha, Tokyo/VCH, Weinheim, New York, 1993.
[3] J.B. Moffat, Metal-Oxygen Clusters. The Surface and Catalytic Properties of Heteropoly Oxometalates, Kluwer/Academic, New York, 2001.
[4] M.I.V. Kozhevnikov, Catalysis by Polyoxometalates, Wiley, Chichester, 2002.
[5] A. Chakrabarti, M.M. Sharma, React. Polym. 20 (1993) 1.
[6] M.M. Sharma, React. Funct. Polym. 26 (1995) 3.
[7] M.A. Harmer, Q. Sun, Appl. Catal., A 221 (2001) 45.
[8] G.A. Olah, G.K.S. Prakash, J. Sommer, Superacids, Wiley, New York, 1985, Chapter 5.
[9] M.A. Harmer, W.E. Farneth, Q. Sun, J. Am. Chem. Soc. 118 (1996) 7708.
[10] B. Török, I. Kiricsi, Á. Molnár, G.A. Olah, J. Catal. 193 (2000) 132.
[11] M.H. Valkenberg, W.F. Hölderich, Catal. Rev.–Sci. Eng. 44 (2002) 321.
[12] A.P. Wight, M.E. Davis, Chem. Rev. 102 (2002) 3589.
[13] J.S. Beck, J.C. Vartuli, W.J. Roth, M.E. Leonowicz, C.T. Kresge, K.D. Schmitt, C.T.W. Chu, D.H. Olson, E.W. Sheppard, S.B. McCullen, J.B. Higgins, J.L. Schlenker, J. Am. Chem. Soc. 114 (1992) 10834.
[14] C.T. Kresge, M.E. Leonowicz, W.J. Roth, J.C. Vartuli, J.S. Beck, Nature 359 (1992) 710.
[15] P.T. Tanev, T.J. Pinnavaia, Science 267 (1995) 865.
[16] P.T. Tanev, T.J. Pinnavaia, Chem. Mater. 8 (1996) 2068.
[17] W. Zhang, T.R. Pauly, T.J. Pinnavaia, Chem. Mater. 9 (1997) 2491.
[18] D.Y. Zhao, J.L. Feng, Q.S. Huo, N. Melosh, G.H. Fredrickson, B.F. Chmelka, G.D. Stucky, Science 279 (1998) 548.
[19] D.Y. Zhao, Q.S. Huo, J.L. Feng, B.F. Chmelka, G.D. Stucky, J. Am. Chem. Soc. 120 (1998) 6024.
[20] S.L. Burkett, S.D. Sims, S. Mann, Chem. Commun. (1996) 1367.
[21] D.J. Macquarrie, Chem. Commun. (1996) 1961.
[22] C.E. Fowler, S.L. Burkett, S. Mann, Chem. Commun. (1997) 1769.
[23] J.H. Clark, D.J. Macquarrie, Chem. Commun. (1998) 853.
[24] S.R. Hall, C.E. Fowler, B. Lebeau, S. Mann, Chem. Commun. (1999) 201.
[25] J.H. Clark, Acc. Chem. Res. 35 (2002) 791.
[26] I.J. Dijs, H.F.L. van Ochten, C.A. van Walree, J.W. Geus, L.W. Jenneskens, J. Mol. Catal. A: Chem. 188 (2002) 209.
[27] E. Cano-Serrano, G. Blanco-Brieva, J.M. Campos-Martin, J.L.G. Fierro, Langmuir 19 (2003) 7621.
[28] S. Shylesh, S. Sarma, S.P. Mirajkar, A.P. Singh, J. Mol. Catal. A: Chem. 212 (2004) 219.
[29] K. Shimizu, E. Hayashi, T. Hatamachi, T. Kodama, Y. Kitayama, Tetrahedron Lett. 45 (2004) 5135.
[30] W.M. Van Rhjin, D.E. De Vos, B.F. Sels, W.D. Bossaert, P.A. Jacobs, Chem. Commun. (1998) 317.
[31] W.D. Bossaert, D.E. De Vos, W.M. Van Rhjin, J. Bullen, P.J. Grobet, P.A. Jacobs, J. Catal. 182 (1999) 156.
[32] M.H. Lim, C.F. Blanford, A. Stein, Chem. Mater. 10 (1998) 467.
[33] I. Díaz, C. Márquez-Alvarez, F. Mohino, J. Pérez-Pariente, E. Sastre, J. Catal. 193 (283) (2000) 295.
[34] I. Díaz, F. Mohino, J. Pérez-Pariente, E. Sastre, Appl. Catal., A 205 (2001) 19.
[35] I. Díaz, F. Mohino, J. Pérez-Pariente, E. Sastre, Appl. Catal., A 242 (2003) 161.
[36] J. Pérez-Pariente, I. Díaz, F. Mohino, E. Sastre, Appl. Catal., A 254 (2003) 173.
[37] D. Das, J.-F. Lee, S. Cheng, J. Catal. 223 (2004) 152.
[38] M. Boveri, J. Agúndez, I. Díaz, J. Pérez-Pariente, E. Sastre, Collect. Czech. Chem. Commun. 68 (2003) 1914.

[39] J.S. Choi, D.J. Kim, S.H. Chang, W.S. Ahn, Appl. Catal., A 254 (2003) 225.
[40] K. Wilson, A.F. Lee, D.J. Macquarrie, J.H. Clark, Appl. Catal., A 228 (2002) 127.
[41] I.K. Mbaraka, D.R. Radu, V.S.-Y. Lin, B.H. Shanks, J. Catal. 219 (2003) 329.
[42] J.G.C. Shen, R.G. Herman, K. Klier, J. Phys. Chem. B 106 (2002) 9975.
[43] S. Koujout, D.R. Brown, Catal. Lett. 98 (2004) 195.
[44] V. Dufaud, M.E. Davis, J. Am. Chem. Soc. 125 (2003) 9403.
[45] R.D. Badley, W.T. Ford, J. Org. Chem. 54 (1989) 5437.
[46] R.G. Herman, F.H. Khouri, K. Klier, J.B. Higgins, M.R. Galler, C.R. Terenna, J. Catal. 228 (2004) 347.
[47] C.W. Jones, M. Tsapatsis, T. Okubo, M.E. Davis, Microporous Mesoporous Mater. 42 (2001) 21.
[48] J.A. Melero, G.D. Stucky, R. van Grieken, G. Morales, J. Mater. Chem. 12 (2002) 1664.
[49] J.A. Melero, R. van Grieken, G. Morales, V. Nuño, Catal. Commun. 5 (2004) 131.
[50] F. Mohino, I. Díaz, J. Pérez-Pariente, E. Sastre, Stud. Surf. Sci. Catal. 142 (2002) 1275.
[51] E. Gutierrez, A.J. Aznar, E. Ruiz-Hitzky, Stud. Surf. Sci. Catal. 41 (1988) 211.
[52] S. Suzuki, K. Tomori, Y. Ono, J. Mol. Catal. 43 (1987) 41.
[53] E. Cano-Serrano, J.M. Campos-Martin, J.L.G. Fierro, Chem. Commun. (2003) 246.
[54] E.F. Vansant, P. Van Der Voort, K.C. Vrancken, Characterization and Chemical Modification of the Silica Surface, Elsevier, Amsterdam, 1997, Chapter 9.
[55] M. Mohai, Surf. Interface Anal. 36 (2004) 828.
[56] M. Mohai, M.I. Bertóti, Surf. Interface Anal. 36 (2004) 805.
[57] S. Evans, R.G. Pritchard, J.M. Thomas, J. Electron Spectrosc. Relat. Phenom. 14 (1978) 341.
[58] R.F. Reilman, A. Msezane, S.T. Manson, J. Electron Spectrosc. Relat. Phenom. 8 (1976) 389.
[59] I.J. Dijs, H.F.L. van Ochten, A.J.M. van der Heiden, J.W. Geus, L.W. Jenneskens, Appl. Catal. A 241 (2003) 185.
[60] D. Margolese, J.A. Melero, S.C. Christiansen, B.F. Chmelka, G.D. Stucky, Chem. Mater. 12 (2000) 2448.
[61] M. Thommes, R. Köhn, M. Fröba, Appl. Surf. Sci. 196 (2002) 239.
[62] N.B. Colthup, L.H. Daly, S.E. Wiberly, Introduction to Infrared and Raman Spectroscopy, Academic Press, Boston, 1990.
[63] L.J. Bellamy, Advances in Infrared Group Frequencies, Chapman and Hall, London, 1968.
[64] E.F. Vansant, P. Van Der Voort, K.C. Vrancken, Characterization and Chemical Modification of the Silica Surface, Elsevier, Amsterdam, 1997, Chapter 9, p. 59.
[65] J. Pande, M.J. McDermott, R.H. Callender, A. Spector, Arch. Biochem. Biophys. 269 (1989) 250.
[66] A.B. Kudryavtsev, S.B. Mirov, L.J. DeLucas, C. Nicolete, M. van der Woerd, T.L. Bray, T.T. Basiev, Acta Crystallogr. D 54 (1998) 1216.
[67] D.W. Sindorf, G.E. Maciel, J. Am. Chem. Soc. 105 (1983) 3767.
[68] G.A. Olah, Acc. Chem. Res. 4 (1971) 240.
[69] B. Chaudhuri, M.M. Sharma, Ind. Eng. Chem. Res. 28 (1989) 1757.
[70] Q. Sun, W.E. Farneth, M.A. Harmer, J. Catal. 164 (1996) 62.
[71] A. Heidekum, M. Harmer, W.F. Hölderich, Catal. Lett. 47 (1997) 243.
[72] M. Fujiwara, K. Kuraoka, T. Yazawa, Q. Xu, M. Tanaka, Y. Souma, Chem. Commun. (2000) 1523.
[73] K. Kurokawa, M. Ohta, K. Sugiyama, H. Miura, Appl. Catal. A 202 (2000) 147.
[74] B. Rác, G. Mulas, A. Csongrádi, K. Lóki, Á. Molnár, Appl. Catal. A 282 (2005) 255.
[75] Reference 8, p. 330.
[76] M. Schneider, K. Zimmermann, F. Aquino, W. Bonrath, Appl. Catal. A 220 (2001) 51.
[77] E.M. Arnett, R.A. Haaksma, B. Chawla, M.H. Healy, J. Am. Chem. Soc. 113 (1986) 4888.
[78] S. Koujout, B.M. Kiernan, D.R. Brown, H.G.M. Edwards, J.A. Dale, S. Plant, Catal. Lett. 85 (2003) 33.
[79] D. Brunel, A. Cauvel, F. Di Renzo, F. Fajula, B. Fubini, B. Onida, E. Garrone, New J. Chem. 25 (2000) 807.
[80] K. Shimizu, E. Hayashi, T. Hatamachi, T. Kodama, T. Higuchi, A. Satsuma, Y. Kitayama, J. Catal. 231 (2005) 131.